

# BioARS: Designing Adaptive and Reconfigurable Bionic Assembly Robotic System with Inchworm Modules

Yide Liu, Donghao Zhao, Yanhong Chen, Dongqi Wang, Zhou Wen, Ziyi Ye, Jianhui Guo, Haofei Zhou, Shaoxing Qu, Wei Yang

**Abstract**— Designing a swarm of robots to address different tasks and adapt to various environments through self-assembly is one of the most challenging topics in the field of robotics research. Here, we present an assembly robotic system with inchworm robots as modules. The system is called BioARS (Bionic Assembly Robotic System). It can either work as a swarm of individual untethered inchworm robots or be assembled into a quadruped robot. The inchworm robots are connected by magnets using a “shoulder-to-shoulder” connecting method, which helps strengthen the magnetic connection. Central pattern generators are used to control the trot gait of the quadruped robot. Our experiments demonstrate that the bionic assembly system is adaptive in that it can pass through confined spaces in the form of inchworms and walk on rough terrain in the form of a quadruped robot. The proposed BioARS, therefore, combines the flexibility of inchworms and the adaptability of quadruped animals, which is promising for application in planetary exploration, earthquake search and rescue operations. We also provide several examples of directions for future research regarding our system.

## I. INTRODUCTION

Recently, bionic robots inspired by animals ranging from insects (such as inchworms [1], bees [2], and cockroaches [3], [4]) to large mammals (such as dogs [5] and humans [6]) have been proposed and attracted enormous attention. Robots inspired by the locomotion of inchworms are flexible and agile [1], [7], [8]. The crawl locomotion of inchworms is converted from the buckling motion of their bodies. Quadruped animals, such as terrestrial vertebrates, possess strong adaptability, which makes them the most dominant animals on land. Quadruped bionic robots have been designed to show high adaptability and ability to move on different landforms [5], [9], [10]. However, it remains challenging to design bionic robots for various environments. For instance, most bionic robot systems are not capable of passing through confined spaces like insects and at the same time walking on rough terrain like quadruped robots.

Assembly and reconfiguration are of special interest in robotic research, ranging from large to small scale and from rigid to soft robotic systems. They can provide modular robots with additional capabilities and functions [11], [12], [13], [14], [15], [16], [17], [18]. For rigid assembly robotic systems, modules are often patterned homogeneously, like atoms in a

All the authors are with the Department of Engineering Mechanics, Zhejiang University, 310027 China (corresponding authors to provide e-mails: haofei\_zhou@zju.edu.cn (Haofei Zhou), squ@zju.edu.cn (Shaoxing Qu)).

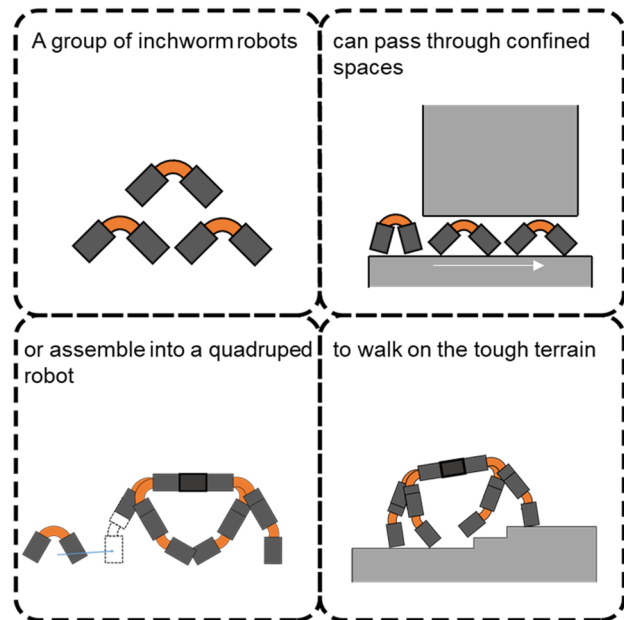


Fig. 1: Design concept of the BioARS (Bionic Assembly Robotic System). The system is a group of inchworm robots. They are small and agile and the system can pass through confined spaces as a swarm of individual robots. When faced with rough terrain, the system can assemble into a quadruped robot. Inchworm robots form the joints of the quadruped robot. Due to the structure of the quadruped robot, the assembled BioARS possesses better landform adaptability.

crystal. Modules can move autonomously. The configuration of the robotic system can be accurately predicted to help the system reconfigure to meet different tasks [11], [12], [16], [17]. Soft assembly robotic systems possess modules with high flexibility and are easy to fabricate [18]. Different from rigid assembly robotic systems, they are usually powered by a pump. The modules are tethered and manually connected. Recently, a type of robotic system containing a swarm of robots with cell-like modules was proposed to imitate living tissues [19], [20]. The behaviors of collective cells were investigated with a focus on cell-scale problems. Overall, assembly robotic systems have high flexibility and adaptability that enable the robotic system to adapt to unpredictable environments and accomplish complex tasks. However, the mobility of assembly

Yide Liu, Donghao Zhao, Yanhong Chen, Dongqi Wang, Haofei Zhou, Shaoxing Qu, and Wei Yang are with the State Key Laboratory of Fluid Power & Mechatronic System, Key Laboratory of Soft Machines and Smart Devices of Zhejiang Provinces, Center for X-Mechanics, Zhejiang University, 310027 China.

and reconfigurable robotic systems is often limited by heavy module design and large assembled size.

We aimed to build an adaptive and reconfigurable bionic robotic system through assembling a swarm of individual modular robots. The lower-level module is an inchworm, while the assembled higher-level robot is a quadruped robot. We refer to it as BioARS (Bionic Assembly Robotic System). The BioARS combines the advantages of both inchworm robots and quadruped robots. It can choose its configuration to adapt to different environments and tasks. The system can pass through confined spaces as a swarm or assemble into a stronger configuration. This is beneficial for complex tasks such as planetary exploration. For instance, one can put a swarm of inchworm robots in place to search the ground. Then they can be assembled into quadruped robots to search rough areas or carry heavy soil samples.

In our design, each quadruped robot consists of eight inchworm robots, serving as its ankles and organs. The inchworm robot is chosen as the module of the robotic system due to the following advantages:

1. Ease of design and fabrication
2. Agility and flexibility
3. Similarity between the buckling motion of an inchworm and the buckling motion of the joints of a quadruped robot.

Compared with designs proposed by Sambot [14] and Fable [16], which can also assemble into a quadruped configuration, the modules of the BioARS are simpler and behave more like an inchworm robot rather than a block or stick. Because of the simple design and lightweight module, the quadruped configuration of the BioARS can contain more modules in each leg than Sambot and Fable’s design (Sambot and Fable: 1, BioARS: 2), giving it more potential for mobility.

In BioARS, each inchworm robot has a hybrid structure composed of a compliant reed connecting two rigid feet. An onboard power control and communication system are embedded to make the inchworm robot untethered and remotely controllable. NdFeB (Neodymium-iron-boron) magnets are embedded at the head, end, and side wings of the inchworm robots to serve as connectors. In the quadruped robot, two inchworm robots connect to form a leg, connected in turn to a cross-shaped rigid body. A connecting method called “shoulder-to-shoulder” is used to make the connection strong and steady. The gait control strategy of the quadruped robot takes inspiration from the CPG (central pattern generator) of vertebrates [21], [22]. In nature, CPGs produce the periodic signals to drive gait patterns. The brain only modulates the CPGs. In this work, the micro-controllers on the inchworm robots serve as the CPG to generate periodic gait signals.

Different species adapt to different environments and have different locomotion ability. Naturally, it takes hundreds of millions of years for a species to evolve to another species to adapt to the environment. However, it only takes inchworm robots a few seconds to assemble into a quadruped animal with the BioARS. The whole system integrates the flexibility of the

inchworm robots and the adaptability to various landforms of the quadruped robot. The configuration of the system could

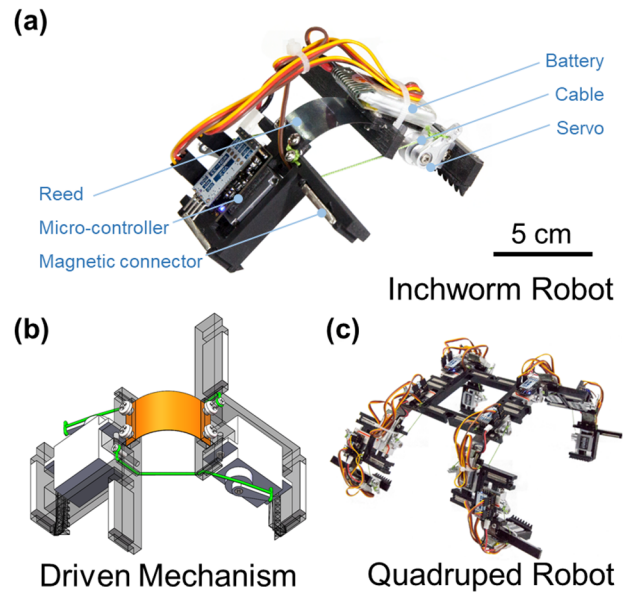


Fig. 2: Design of the BioARS (a) Module: inchworm robot. (b) CAD model of the driving mechanism of the inchworm robot. (c) Assembled robot: quadruped robot.

potentially switch between small and large, light and heavy. Since the BioARS system can cover both confined spaces and rough terrain, it is expected that such a system holds potential for planetary exploration and earthquake search and rescue.

## II. DESIGN AND FABRICATION

An assembly robotic system includes a swarm of robots as modules, which bind with each other through connectors. The assembly process of the system is generally task-oriented and the assembled robot has better adaptability and more functions compared with a single module. Therefore, the design and fabrication of an assembly robotic system is always focused on the module, the connector, and the assembled robot.

In the BioARS, the inchworm robot is the basic module. A micro-controller and battery are attached to the inchworm robots, making the entire system untethered. Magnets are used to connect the inchworms. We use a “shoulder-to-shoulder” connecting method to prevent failure due to large bending moment during assembly and walking.

The assembled robot is a quadruped which consists of eight inchworm robots and a rigid body. To achieve gait control of the assembled quadruped robot, a master computer is introduced and a four-level control strategy is proposed.

### A. Inchworm Robot

Figs. 2a and 2b show the sketch and CAD model of the inchworm robot. The body of the inchworm is composed of two rigid feet and a compliant reed. The rigid feet are made of resin printed with a multi-material 3D printer (Object 260 Connex 3, Stratasys). The reed is made from manganese steel with excellent resilience. Each foot is attached with a servo and the servo is connected to the other foot with a cable. The

servo motors are driven by signals with different frequencies from a custom-designed micro-controller and powered by a 3.7 V lithium-polymer battery.

The driving mechanism of the inchworm robot is formed by the two servos and the compliance reed. The buckling motion of the inchworm robot is driven by the rotation of the servo motors and pulling of the cables. The restoring force is supplied by the compliant reed. Hooks are aligned at the bottom of the front and back feet to create asymmetric friction. The asymmetric friction force transfers the buckling motion into the crawl locomotion.

### B. Magnetic connector

When we designed the connector for this assembly robotic system, we considered the geometric size, weight, connecting force, ease of use, and other factors. Commercial NdFeB magnet was chosen as the material for the connector due to its light weight, small size, and strong connecting force. Magnetic connectors do not require manual assembly or orientation, which can simplify the assembly process. In this design, the weight of a magnet is about 5.6g and the geometric size is 25mm×10mm×3mm. One inchworm robot has four magnets, two on the ends of the feet and two on the side wings.

Here we want to particularly discuss the connecting method we applied in the bionic robotic system, which we call “shoulder-to-shoulder” (Fig. 3). Compared with the conventional method of magnetic connection we call “head-to-head”, “shoulder-to-shoulder” can significantly increase the connecting moment. Moreover, it can shorten the arm of the resistance during the quadruped robot’s standing motion and make the structure of the quadruped robot more compact. In section 3.2, we offer characterizations and comparisons of the connecting methods.

### C. Quadruped Robot

Fig. 3 shows the photo of the assembled quadruped robot in the lying configuration. Figs. 2(c) and 4(a) show the robot in the standing configuration. The standing quadruped robot is an X-shaped robot with dimensions of 0.308 m(width), 0.230 m(length) and 0.156 m(height) with a cross-shaped rigid body at the center. The rigid body is created by 3D printing and eight NdFeB magnets are embedded around it (Fig. 4(b)). The total weight of the quadruped robot is 0.8 kg.

Fig.5 shows the assembly and standing process in stages. First, eight inchworm robots connect to the rigid body in order (in the experiment, all the inchworm robot were placed manually). After connecting, the standing command is sent, and all the inchworm robots stop crawling. As eight inchworm robots group to form four legs, four shin inchworm robots buckle first to shorten the arm of the resistance force. This configuration is called pre-standing. Finally, four thigh inchworm robots start buckling to make the quadruped robot stand up completely.

### D. Gait Control

Since the quadruped robot is assembled from eight individual inchworm modules which are only equipped with wireless communication devices, the gait of the quadruped

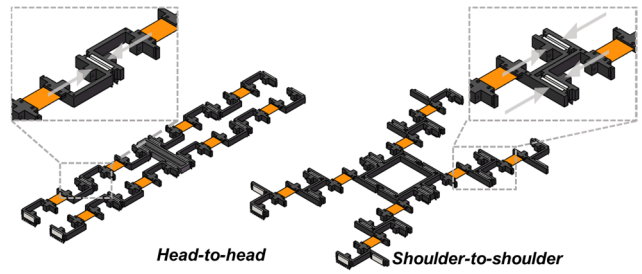


Fig. 3: Sketches of the “head-to-head” and “shoulder-to-shoulder” connecting methods.

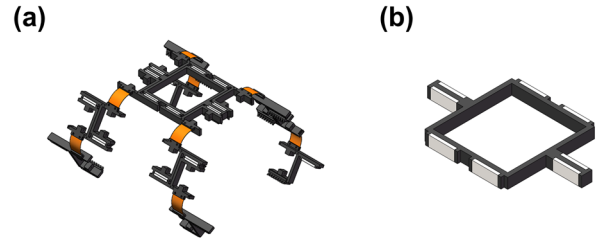


Fig. 4: (a) Sketch of the quadruped robot in standing configuration. (b) Sketch of the cross-shaped rigid body. Eight magnetic connectors are embedded around the rigid body.

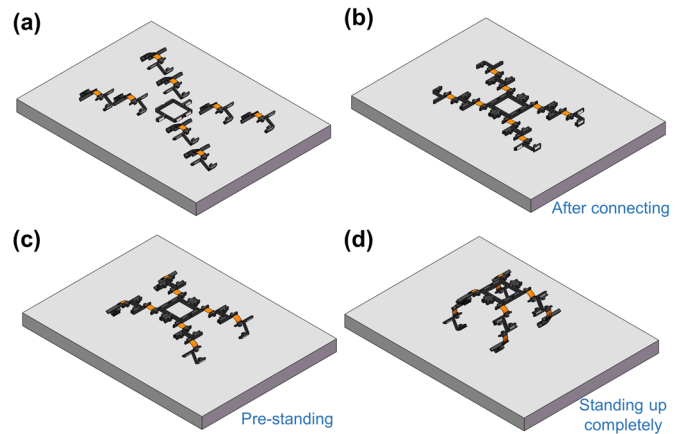


Fig. 5: Assembly and standing process of the quadruped robot. (a)-(b) Eight inchworm robots connect to the cross-shaped rigid body in order. (c) Pre-standing configuration: four shin joints buckle to shorten the arm of the resistance force. (d) Four thigh inchworms buckle and the quadruped robot stands up completely. For more details, see the supplementary video.

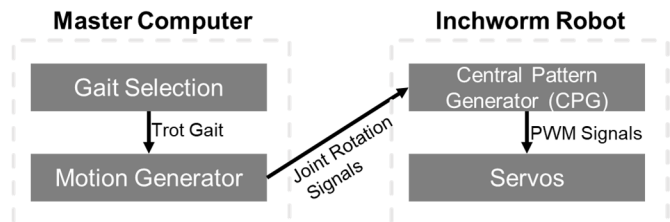


Fig. 6: Four-level gait control architecture of the quadruped. The first level (gait selection) chooses the gait of the quadruped robot. The second level (motion generator) generates the rotation cycles for each joint based on the selected gait. Then the joint rotation signals are sent to the inchworm robots respectively. The third level (central pattern generator) generates PWM signals based on the joint rotation signals. The last level is the servo, which executes the PWM signals to make the quadruped robot perform the selected gait.

robot must be handled on different levels. We used a master computer to communicate with all eight inchworms and control the gait of the quadruped robot.

The architecture of the gait control consists of four levels (Fig. 6). The first level is gait selection, where the gait of the quadruped robot is selected. In this work, we adopt the trot gait of the quadruped robot as an example. Based on the selected trot gait, the second level (motion generator) produces eight individual rotation cycles for each joint of the quadruped robot. Rotation cycles of each joint for trot gait are predefined in the master computer (Fig. 7(c)). Then the master computer sends all the rotation cycles to the receivers of the inchworm robots (Fig. 7(b)). The third level takes place on the onboard controller of the inchworm robots. After receiving the rotation signals, the micro-controllers of the individual inchworm robots serve as CPGs to generate periodic PWM signals based on the joint rotation signals. The transfer relationship is predefined in the onboard controller of the modules. The servos execute the PWM signals to ensure that the whole quadruped robot performs a periodic trot gait.

### III. EXPERIMENTAL RESULTS

In this part, we characterize the metrics of individual modules including their velocity and turning radius. We illustrate the assembly procedure and propose a “shoulder-to-shoulder” inchworm connection method to resist bending moment in the assembled configuration. Three main tests were performed: individual inchworms assembling into a quadruped robot which stands on four legs and walks; inchworms passing through confined spaces; and the quadruped robot climbing obstacles.

#### A. Experiments with the inchworm robot

We first demonstrate the locomotion of a single inchworm robot. In BioARS, the time required for gathering and assembling is determined by how quickly and nimbly the modules can move. To transfer the buckling motion of the inchworm robot into crawl locomotion, the inchworm robot was set on a platform covered with nylon cloth. The inchworm robot rotates between two angles, the minimum rotation angle  $\alpha_1$  and the maximum rotation angle  $\alpha_2$  (Fig. 8(a)). The maximum rotation angle  $\alpha_2$  is set as  $120^\circ$ ,  $150^\circ$ , and  $180^\circ$ . The frequency of buckling motion  $f$  is set as 1 Hz and 2 Hz. The minimum rotation  $\alpha_1$  ranges from  $90^\circ$  to  $180^\circ$ . The velocity of the inchworm robot is recorded in Fig. 8 (b).

The turning test of the inchworm robot mainly focused on the turning radius  $R_{turning}$  (Fig. 8(c)). The buckling motion of the inchworm robot is driven by the rotation of the pair of servo motors and through pulling the cables. During the turning, we only actuate one servo to pull the cable. Thus, the inchworm robot will buckle asymmetrically (Fig. 8(d)). The experiment results show that the minimum turning radius is about 80cm while the actuated servo is set as  $\alpha_1 = 90^\circ$ .

#### B. Characterizations of the magnetic connector

Previous work has proved that the “head-to-head” connection is capable of resisting tensile load and shearing load [18]. However, this connecting method cannot meet the

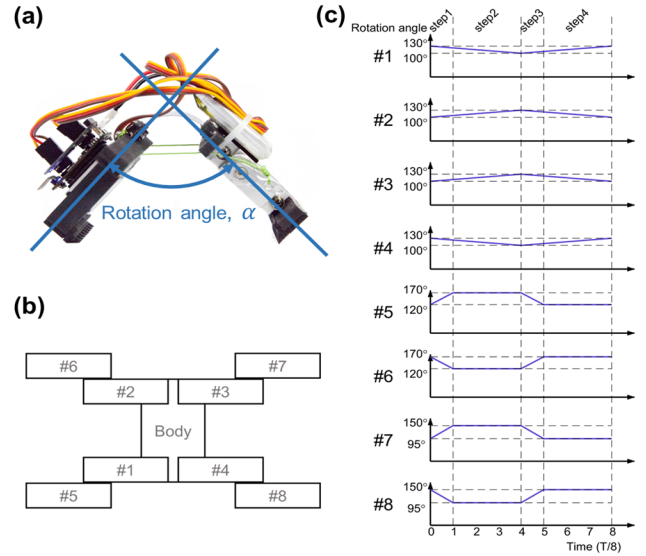


Fig. 7: Gait design of the quadruped robot. (a) Definition of the rotating angle  $\alpha$  in inchworm robot. (b) Notation of the quadruped robot. (c) Control signals of the eight inchworm robots. The combined motions of the inchworm robots make the quadruped robot perform trot gait walking.

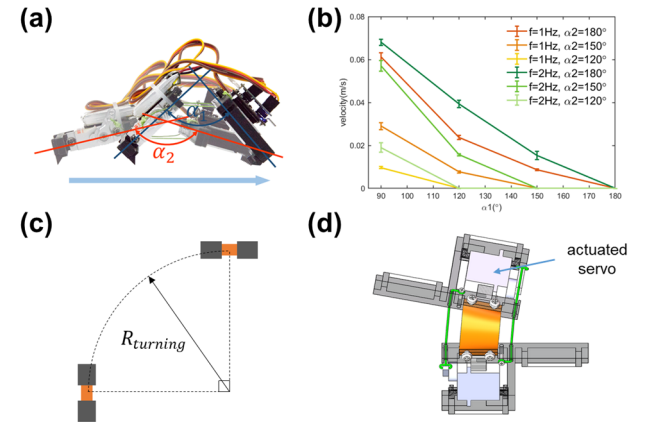


Fig. 8: (a) The rotation angle of the inchworm varies within two fixed angles  $\alpha_1$  and  $\alpha_2$ . (b) Velocity of the inchworm robot measured in different test conditions. (c) Definition of the turning radius  $R_{turning}$ . (d) CAD model of the turning inchworm robot. The inchworm robot turns to the right as the front servo is actuated.

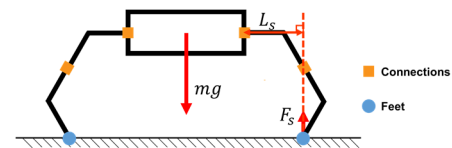


Fig. 9: Quasi-static model of the failure bending moment calculation. The maximum failure bending moment occurs at the connection between the body and the thigh.

requirement of the high bending moment resistance in our model. As the quadruped robot stands and walks, the joints of the quadruped robot are under large bending force, and the failure bending moment of the magnetic connection is relatively large.

We composed a quasi-static analytical model to calculate the failure bending moment of the magnetic connection (Fig. 9). During the quadruped robot standing process, gravity is

distributed equally on the four feet and the support force  $F_s$  at each foot is:

$$F_s = m \times g/4$$

where  $m$  is the mass of the quadruped robot and  $g = 9.8\text{m/s}^2$  is the gravity acceleration. The maximum failure bending moment occurs at the thigh-body connection. The failure bending moment all comes from the support force  $F_s$  at the feet, and the arm of the supported force is  $L_s$ . So, the failure bending moment  $M_{bending}$  of the magnetic connection can be calculated as:

$$M_{bending} = F_s \times L_s = mgL_s/4$$

In this design, the total mass of the quadruped robot  $m$  is 0.8 kg and the length of the force arm  $L_s$  ranges from 0.08 m to 0.15 m. Consequently, the maximum failure bending moment  $M_{bending}$  is approximately 0.3 Nm.

We performed uniaxial pulling measurements to characterize the attractive force of different pairs of magnetic connections against tensile and shear load (Figs. 10(a) and 10(b)). A failure bending moment test was designed to compare and characterize the “head-to-head” and “shoulder-to-shoulder” connecting methods (Fig. 10(c)).

Comparing the results of the tests of these two connecting methods, the failure bending moment resistance of the latter test is much higher than the former. This proves that the “shoulder-to-shoulder” connecting method can promote the failure bending moment resistance of the magnetic connections. Moreover, the “shoulder-to-shoulder” connecting method can perfectly cover the maximum failure bending moment of the BioARS.

### C. Experiments with the quadruped robot

Here we perform an experiment to demonstrate the working process of the assembled BioARS (Fig. 11). The experiment includes three processes: assembly (with manual placement and remote control), standing, and walking. First, eight inchworm robots gather together around the rigid body and connect to it in order. When the magnetic connectors are close enough (about 4cm, depending on the friction), the magnetic force will pull the pair of magnets together. Thus, it is unnecessary for the inchworm robots to align precisely.

After the quadruped robot assembled, we turned on the master computer to control the inchworm robots. The inchworm robots stopped moving and the quadruped robot was like lying on the ground. During this step, the master computer was synchronizing all the onboard micro-controllers of the inchworm robots for the walking process. Then, following the gait control strategy we designed, the quadruped robot stood up and began walking.

The locomotion ability of the quadruped robot was tested on both the nylon cloth surface and an ordinary wooden floor. The frequency of the trot gait walking is fixed as 2 Hz and the average velocities are 0.12m/s and 0.1m/s, respectively. Compared with the single inchworm robot under the same

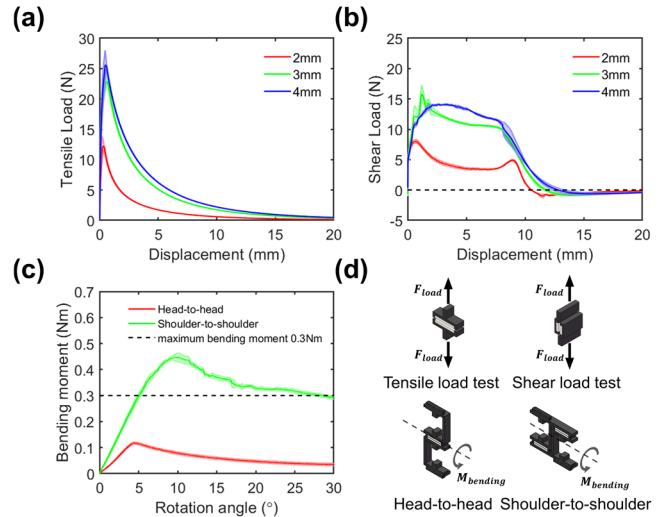


Fig. 10: Characterizations of the magnetic connections. (a) Tensile load test: attraction force of three pairs of magnetic connections (length: 25mm, width: 10mm, thickness: 2mm/ 3mm/ 4mm) against tensile. (b) Shear load test: attraction force of three pairs of magnetic connections against shear. (c) Magnetic connection test: comparison of the “head-to-head” and “shoulder-to-shoulder” connecting methods under bending moment (length: 25mm, width: 10mm, thickness: 3mm). (d) Schematic illustrations of the tests.

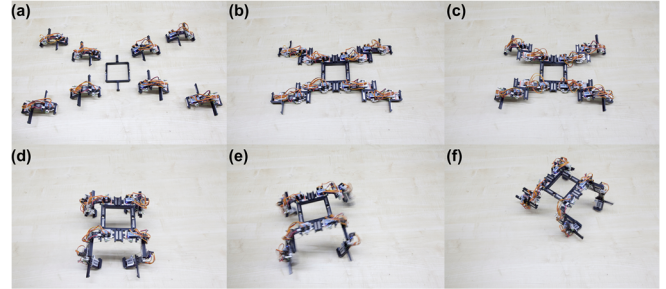


Fig. 11: (a)-(b) Assembly Process: eight inchworm robots assemble into a quadruped robot (with manual placement and remote control). (c)-(d) Standing process: quadruped robot stands up with two steps: 1. four inchworm robots as shin joints buckle first and the quadruped robot switches to pre-standing configuration; 2. four inchworm robots as thigh joints buckle next and the quadruped robot stands up completely. (e)-(f) Walking process: quadruped robot walks to the right in trot gait.

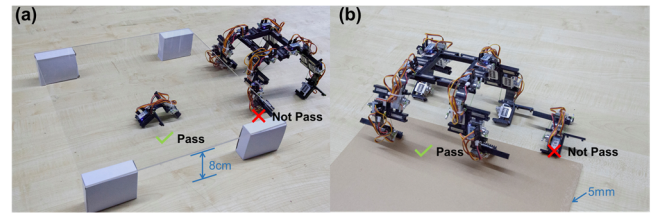


Fig. 12: (a) Confined space test. Inchworm robots can pass through the 8cm-high confined space while the quadruped robot is too large. (b) Obstacle climbing test. The quadruped robot could climb the 5mm-high obstacle while the inchworm robot could not.

conditions, the maximum velocity of the quadruped configuration is 70% faster.

We performed the confined space passing experiment on both the inchworm robot and quadruped robot (Fig. 12(a)). The result shows that the inchworm can pass through an 8cm-high path while the quadruped robot cannot, demonstrating that the small size and flexibility of the inchworm robot is

beneficial to the mobility of the bionic robotic system because the whole system can pass through confined spaces as a swarm of inchworm robots.

The test of the climbing ability of the quadruped robot is shown in Fig. 12(b). The whole system can assemble into the quadruped robot configuration to climb a 5mm-high step while the individual inchworm robots could not. Even though a step height of 5mm is less than ideal for a quadruped robot of this size, it demonstrates the adaptability of the BioARS to rough terrain benefiting from the quadruped configuration.

#### IV. DISCUSSION AND CONCLUSION

We designed a bionic assembly robotic system (BioARS) with inchworm robots as modules. The assembly configuration of the system is a quadruped robot. Onboard power and control systems are integrated to make the inchworm robot module untethered and flexible. To control the gait of the assembled quadruped robot, a master computer generates the gait and joint rotation signals. The individual onboard controllers serve as central pattern generators to control the periodic gait of the quadruped robot. We performed a set of experiments to demonstrate our purpose in building such a robotic system. As a bionic robotic system, it incorporates the merits of both the inchworm and the quadruped animal. The BioARS can pass through confined spaces as a swarm of inchworm robots or climb obstacles as a quadruped robot.

Our experimental results also shed light on several open questions to be addressed:

1. The robotics system cannot assemble automatically. Human assistance plays an important role in the gathering process (manual placement) and assembly process (remote control) of the robotic system. To solve this problem, navigation sensors should be integrated into the inchworm robots to achieve an autonomous robotic system.
2. The magnetic connectors are difficult to disconnect. The quadruped robot cannot disassemble into a swarm of inchworm robotics. This drawback seriously affects the flexibility of the robotic system. To achieve the functionality of disconnecting the magnetic connector, an extra actuator can be added at the side wing. However, there is a trade-off between the connecting force and the disconnecting force. As we analyzed in section III.b, for our system, the connecting force depends on the weight of the system. If extra actuators are added to help break the connector, the system will be heavier and the induced connecting force will be larger. Thus, to add actuators for disconnection, the weight of the system should be reduced first. Shape-memory alloy could be chosen as the actuator for disconnection due to its large force and light weight.
3. The mobility of the robotics system is less than ideal, both for the inchworm robots and the quadruped robot, in the aspects of velocity, turning ability, and climbing adaptability. There are some redundant parts in the

mechanical design of the system which lead to the robotics system being large and heavy. Since there is a trade-off between the strength and the resilience of the reed, it is challenging to improve the metric of step height of the present system. We plan to develop a second generation of the bionic assembly robotic system with lighter material and a more compact design.

For the next step, we are considering improvements to our system based on the above analysis. The ongoing research focuses on refining the mechanical design of the inchworm robot and equipping the inchworm robot with more sensors. We plan to narrow the size of the inchworm robot to the centimeter scale. The control strategy of the current system will be retained, but the servos will be replaced by smart material actuators such as shape-memory alloy and a piezoelectric bending actuator.

#### ACKNOWLEDGMENT

The authors thank Hejinsheng Cao for his help and suggestions on this work. This work is supported by the National Natural Science Foundation of China (Nos 11525210, 91748209), Zhejiang Province Key Research and Development Project (No. 2020C05010), the Fundamental Research Funds for Central Universities (No. 2020XZZX005-02), and Zhejiang University through "Hundred Talents Program".

#### REFERENCES

- [1] J.-S. Koh and K.-J. Cho, "Omegabot: Biomimetic inchworm robot using SMA coil actuator and smart composite microstructures (SCM)," presented at the IEEE International Conference on Robotics and Biomimetics (ROBIO), 2009.
- [2] R. J. Wood, "The first takeoff of a biologically inspired at-scale robotic insect," *Ieee Transactions on Robotics*, vol. 24, no. 2, pp. 341-347, 2008.
- [3] A. T. Baisch, O. Ozcan, B. Goldberg, D. Ithier, and R. J. Wood, "High speed locomotion for a quadrupedal microrobot," *International Journal of Robotics Research*, vol. 33, no. 8, pp. 1063-1082, 2014.
- [4] J. M. Morrey, B. Lambrecht, A. D. Horchler, R. E. Ritzmann, and R. D. Quinn, "Highly mobile and robust small quadruped robots," presented at the IEEE/RSJ International Conference on Intelligent Robots and Systems (IROS), 2003.
- [5] M. Raibert, K. Blankespoor, G. Nelson, and R. J. I. P. V. Playter, "Bigdog, the rough-terrain quadruped robot," *IFAC Proceedings Volumes*, vol. 41, no. 2, pp. 10822-10825, 2008.
- [6] K. Kaneko, K. Harada, F. Kanehiro, G. Miyamori, and K. Akachi, "Humanoid robot HRP-3," presented at the IEEE/RSJ International Conference on Intelligent Robots and Systems (IROS), 2008.
- [7] S. M. Felton, M. T. Tolley, C. D. Onal, D. Rus, R. J. Wood, and Ieee, "Robot Self-Assembly by Folding: A Printed Inchworm Robot," presented at the IEEE International Conference on Robotics and Automation (ICRA), Karlsruhe, GERMANY, 2013.
- [8] W. Wang, J. Y. Lee, H. Rodrigue, S. H. Song, W. S. Chu, and S. H. Ahn, "Locomotion of inchworm-inspired robot made of smart soft composite (SSC)," *Bioinspiration & Biomimetics*, vol. 9, no. 4, p. 046006, 2014.
- [9] Y. Fukuoka, H. Kimura, and A. H. Cohen, "Adaptive dynamic walking of a quadruped robot on irregular terrain based on biological concepts," *International Journal of Robotics Research*, vol. 22, no. 3-4, pp. 187-202, 2003.
- [10] H. Kimura, Y. Fukuoka, and A. H. Cohen, "Adaptive dynamic walking of a quadruped robot on natural ground based on biological concepts," *International Journal of Robotics Research*, vol. 26, no. 5, pp. 475-490, 2007.

- [11] S. Murata, E. Yoshida, A. Kamimura, H. Kurokawa, K. Tomita, and S. Kokaji, "M-TRAN: Self-reconfigurable modular robotic system," *Ieee-Asme Transactions on Mechatronics*, vol. 7, no. 4, pp. 431-441, 2002.
- [12] B. Salemi, M. Moll, W.-M. Shen, and Ieee, "SUPERBOT: A deployable, multi-functional, and modular self-reconfigurable robotic system," presented at the IEEE/RSJ International Conference on Intelligent Robots And Systems (IROS), 2006.
- [13] M. Yim *et al.*, "Modular self-reconfigurable robot systems [grand challenges of robotics]," *IEEE Robotics & Automation Magazine*, vol. 14, no. 1, pp. 43-52, 2007.
- [14] H. Wei, Y. Cai, H. Li, D. Li, and T. Wang, "Sambot: A self-assembly modular robot for swarm robot," presented at the IEEE International Conference on Robotics and Automation (ICRA), 2010.
- [15] J. Davey, N. Kwok, and M. Yim, "Emulating self-reconfigurable robots-design of the SMORES system," presented at the 2012 IEEE/RSJ International Conference on Intelligent Robots and Systems, 2012.
- [16] M. Pacheco, M. Moghadam, A. Magnússon, B. Silverman, H. H. Lund, and D. J. Christensen, "Fable: Design of a modular robotic playware platform," presented at the 2013 IEEE International Conference on Robotics and Automation, 2013.
- [17] J. W. Romanishin, K. Gilpin, and D. Rus, "M-blocks: Momentum-driven, magnetic modular robots," in *2013 IEEE/RSJ International Conference on Intelligent Robots and Systems*, 2013, pp. 4288-4295: IEEE.
- [18] S. W. Kwok *et al.*, "Magnetic Assembly of Soft Robots with Hard Components," *Advanced Functional Materials*, vol. 24, no. 15, pp. 2180-2187, 2014.
- [19] S. G. Li *et al.*, "Particle robotics based on statistical mechanics of loosely coupled components," *Nature*, vol. 567, no. 7748, p. 361, 2019.
- [20] H. Xie *et al.*, "Reconfigurable magnetic microrobot swarm: Multimode transformation, locomotion, and manipulation," *Science Robotics*, vol. 4, no. 28, p. eaav8006, 2019.
- [21] H. Haken, J. A. S. Kelso, and H. Bunz, "A Theoretical-Model of Phase-Transitions in Human Hand Movements," *Biological Cybernetics*, vol. 51, no. 5, pp. 347-356, 1985.
- [22] C. J. Liu, Q. J. Chen, and D. W. Wang, "CPG-Inspired Workspace Trajectory Generation and Adaptive Locomotion Control for Quadruped Robots," *Ieee Transactions on Systems Man and Cybernetics Part B-Cybernetics*, vol. 41, no. 3, pp. 867-880, 2011.